Integrated Optimal Design of a Smart Microgrid With Storage

Remy Rigo-Mariani, Bruno Sareni, Xavier Roboam

Integrated Optimal Design of a Smart Microgrid With Storage

Remy Rigo-Mariani, Bruno Sareni, and Xavier Roboam, *Member, IEEE*

***Abstract*—In this paper, we investigate a design approach aiming at simultaneously integrating the energy management and the sizing of a small microgrid with storage. We particularly underline the complexity of the resulting optimization problem and how it can be solved using suitable optimization methods in compliance with relevant models of the microgrid. We specifically show the reduction of the computational time allowing the microgrid simulation over long time durations in the optimization process in order to take seasonal variations into account. The developed approach allows performing many optimal designs in order to find the appropriate price context that could favor the installation of storage devices.**

***Index Terms*—Dynamic programming, efficient global optimization, evolutionary algorithms, Kriging, linear programming, smart grid, microgrid, sizing, optimal dispatching.**

I. Introduction

WITH THE development of decentralized power stations based on renewable energy sources, distribution networks have strongly evolved to more meshed models [1]. Corresponding architectures can be considered as an association of various "microgrids" both consumer and producer that have to be run independently while granting the global balance between load and generation. Smarter operations now become possible with developments of energy storage technologies and evolving price policies [2]. Those operations would aim at reducing the electrical bill taking account of consumption and production forecasts as well as the different fares and possible constraints imposed by the power supplier [3]. This paper deals with a microgrid devoted to a set of industrial buildings and factories. It includes photovoltaic (PV) production and a storage unit composed of high speed flywheels (FW). The main objective is to develop an original sizing procedure that integrates the management strategy. As illustrated in Fig. 1 a traditional sequential approach would aim at successively optimizing the design and the power dispatching. Using an integrated bi-level procedure allows finding the best compromise between the investment costs and the benefits resulting from the optimal use of the system [1]. In such a method the management loop would have to be simulated over a long period of time for every tested design point generated by the sizing loop. It could lead to prohibitive CPU times. To face this problem, we will show how it can be solved using suitable optimization methods in compliance with relevant models of the microgrid. After describing the power flow model of the system in Section II, the Section III presents several optimization methods in order to simulate the optimal management of the system. It is based on an offline scheduling aiming at minimizing the electrical bill for the day ahead. Note that in real time an on-line procedure adapts the power flows in order to correct the errors between forecasts and actual measurements work [5]. Such control strategy based on the on-line adaptation of off-line optimal references has been extensively studied in the literature (e.g., [6]–[8]) and is not the subject of this work. In particular, a fast optimization approach based on Mixed Integer Linear Programming (MILP) and on a linear model of the microgrid is introduced in order to reduce the CPU time of the power flow dispatching. In Section IV a second optimization level is presented. It consists in determining the optimal design of the microgrid with regard to the energy costs computed over a complete year in order to take seasonal variations into account. Section V presents the results obtained with different price policies aiming at finding the context that could favor the installation of a storage unit.

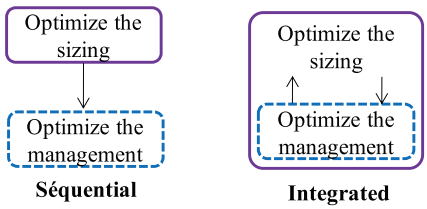

Fig. 1. Coupling between sizing and management loops.

II. Model of the Microgrid

A. Power Flow Model of the Microgrid

Among many other possible topologies, the particular microgrid structure shown in Fig. 2 has been selected by the leader of the ‘’smart ZAE” project (CofelyIneo- GDF Suez). All the microgrid components are connected though a common DC bus. In order to limit the systemic design process complexity, voltages and currents are not represented and only active

R. Rigo-Mariani is with the Department of Electrical Engineering, University of Washington, Seattle, WA 98185 USA (e-mail: rigor@uw.edu)
B. Sareni and X. Roboam are with the Laboratory on Plasma and Conversion of Energy, Université de Toulouse, Toulouse 31071, France (e-mail: sareni@laplace.univ-tlse.fr, roboam@laplace.univ-tlse.fr).

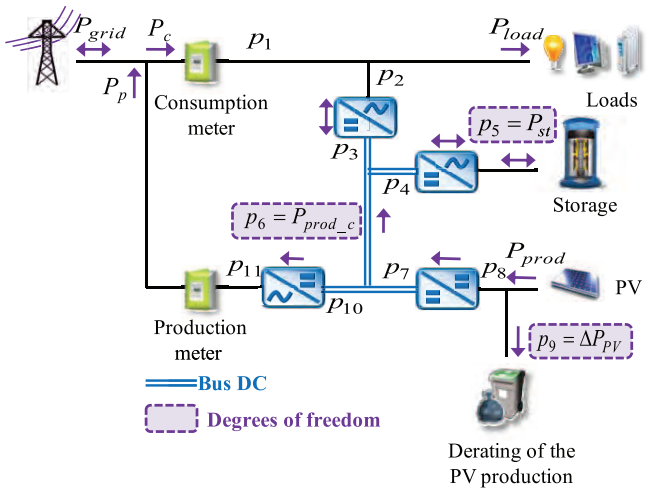

Fig. 2. Power flow model of the studied microgrid.

power flows are considered. In the rest of the paper the instantaneous values are denoted as $p_i(t)$ while the profiles over the periods of simulation are written in vectors $\mathbf{p_i}$. A nomenclature of the main used symbols is given on Table I. Note that only the relevant variables $\mathbf{p_i}$ related to the power management are explained in the text. Due to the grid policy, several constraints have to be fulfilled at each time step t. The power $P_c(t)$ through the consumption meter and $P_p(t)$ through the production meter have to remain mono-directional. $P_{prod\_c}(t)$ has to be positive to avoid illegal use of the storage, flywheels cannot discharge themselves through the production meter. A particular attention is paid to the grid power $P_{grid}(t)$ which should comply with requirements possibly set by the power supplier $P_{grid\_min}(t)$ and $P_{grid\_max}(t)$.

The equations between all power flows are generated using the graph theory and an incidence matrix [10]. As illustrated in Fig. 2, three degrees of freedom are required to manage the whole system knowing production and consumption:

- $p_5(t) = P_{st}(t)$: the power flowing from/to the storage unit (defined as positive for discharge power)
- $p_6(t) = P_{prod\text{-}c}(t)$: the power flowing from the PV arrays to the common DC bus
- $p_9(t) = \Delta P_{PV}(t)$: denotes the possibility to decrease the PV production (MPPT° degradation) in order to fulfill grid constraints, in particular when the power supplier does not allow (or limits) the injection of the PV production into the main grid (p_9 is normally set to zero).

B. Efficiencies of the Microgrid Components

A first model (qualified as "fine model") is defined taking account of power converters efficiencies (typically 98 %) and storage losses. Flywheel losses are computed versus the state of charge *SOC* (in %) and the power P_{st} using a function $P_{loss}(SOC)$ and calculating the efficiency with a fourth degree polynomial $\eta_{FW}(P_{st})$ (see (1)). Both P_{loss} and η_{FW} functions are extracted from measurements provided by the manufacturer (Levisys). Another coefficient K_{FW} (in kWh/h) is also introduced to estimate the self-discharge of the flywheels when they are not used (see (2)). Once the overall efficiency

TABLE I
LISTS OF THE MAIN USED SYMBOLS

Symbol	Quantity	Unit
P_{load}	Consumed power	kW
P_{prod}	Solar PV production	kW
P_c	Power through the consumption meter	kW
P_p	Power through the production meter	kW
P_{st}	Power flowing from/to the storage unit	kW
P_{FW}	Power of the flywheel with losses	kW
P_{st_min} , P_{st_max}	Lower and upper bounds for P_{st}	kW
E_{FW}	Maximum stored energy in the storage unit	kWh
SOC	State of charge of the storage unit	%
SOC_{min} , SOC_{max}	Lower and upper bounds for the SOC level	%
P_{PV}	Nominal power of the PV generator	kWc
P_s	Subscribed power	kVA
$P_{prod\text{-}c}$	Amount of solar production self consumed	kW
ΔP_{PV}	Deratedsolar production	kW
P_{grid}	Power flowing from/to the main grid	kW
P_{grid_min} , P_{grid_min}	Lower and upper bounds for P_{grid}	kW
C_c , C_p	Cost for consumed and produced energies	c€/kWh
C_{ex}	Penalty cost due to the exceeding of P_s	€/h
t	Time step	h
$\mathbf{P_{ref}}$	Matrix/vector with decision variables	-
$C(\mathbf{P_{ref}})$	Daily cost to be minimized	€
$\mathbf{C_{nl}}$	Vector with the nonlinear constraints	-
C_{op} , C_{inst}	Operating and investment costs	k€
K_{der}	Derated consumption	%
$K_{\%}$	Increment of purchased costs	%
C_{der_f} , C_{der_v}	Retribution for the derated consumption	-
TRI	Time of return on investment	years
TCO	Total cost of ownership	k€

is computed, the true power P_{FW} associated with the flywheel is calculated as well as the *SOC* evolution using the maximum stored energy E_{FW} (100 kWh in the initial situation), the time step Δt (typically 1 hour for the off-line optimization) and the control reference P_{st}. Due to the bidirectional characteristics of static converters and especially with the flywheels efficiency, the overall system is intrinsically nonlinear and suitable methods have to be used to solve the optimal power dispatching problem.

$$\begin{cases} P_{st}(t) < 0 \rightarrow P_{FW}(t) = P_{loss}(SOC(t)) + P_{st}(t) \times \eta_{FW}(-P_{st}(t)) \\ P_{st}(t) > 0 \rightarrow P_{FW}(t) = P_{loss}(SOC(t)) + P_{st}(t)/\eta_{FW}(P_{st}(t)) \end{cases} \tag{1}$$

$$\begin{cases} P_{st}(t) \neq 0 \rightarrow SOC(t+\Delta t) = SOC(t) - \dfrac{P_{FW}(t) \times \Delta t}{E_{FW}} \times 100 \\ P_{st}(t) = 0 \rightarrow SOC(t+\Delta t) = SOC(t) - \dfrac{K_{FW} \times \Delta t}{E_{FW}} \times 100 \end{cases} \tag{2}$$

III. POWER FLOW OPTIMIZATION IN THE MICROGRID

A. Optimal Power Dispatching Based on the Fine Model

The power dispatching strategy lies on a classical approach [9] that aims at minimizing the electrical bill for the day ahead. Prices of purchased and sold energy are assumed to be time dependent with instantaneous values respectively denoted as $C_c(t)$ and $C_p(t)$. The time scheduling period is one day discretized on a one hour basis within which the variables are considered to be constant. References of the power flows associated with the degrees of freedom over this period are computed in a vector $\mathbf{P_{ref}}$ of 72 elements (i.e., the total

number of unknowns in the corresponding optimization problem is 3x24). An additional constraint is considered ensuring the same storage level $SOC = 50\%$ at the beginning and at the end of the scheduling period. Once $\mathbf{P_{ref}}$ is determined, all the other power flows are computed from the forecasted values of consumption and production. Then P_c and P_p are known to estimate the balance between purchase and sale. Thus, the energy cost function is calculated as in (3) with the purchase and sold costs. Note that P_s (in kVA) is the power contracted with the power supplier and define a limit for a maximum demand during the billing period. The amount of penalties resulting from the exceedings of P_s (in kVA) are computed using a coefficient C_{ex} expressed in €/h (euros by hours of exceedings).

$$C(\mathbf{P_{ref}}) = \sum_{t=0}^{24\text{h}} P_c(t) \times C_c(t) - P_p(t) \times C_p(t) + \delta(t) \times C_{ex}$$
$$\text{with } \begin{cases} \delta(t) = 0 & \text{if } P_c(t) < P_s \\ \delta(t) = 1 & \text{if } P_c(t) > P_s \end{cases} \quad (3)$$

Due to the nonlinear relations in the fine microgrid model, only nonlinear optimization methods under constraints can be used for solving the power flow dispatching problem. We remind that those methods have to take account of possible constraints on the main grid in addition to the energy cost minimization. For solving such problem several approaches have been proposed in earlier works [5] and [11]:

- Classical nonlinear programming methods and especially the trust region algorithm (TR) [12]
- Stochastic optimization methods like particle swarm optimization (PSO) [13] or evolutionary approaches, especially the clearing algorithm (CL) [14] with a niching mechanism
- Dynamic Programming (DP) [15] which consists in a step by step minimization with regard to the storage state of charge (*SOC*) levels on the overall range (i.e., 0%-100%) with a given accuracy ΔSOC. In particular, a self-adaptive version has been developed in [11] with the aim of improving the compromise in terms of solution accuracy and computational cost.

B. Fast Power Dispatching Based on a Coarse Linear Model

In order to reduce the computational time required for the power flow dispatching in the microgrid, a fast optimization procedure has been proposed in [16] and [17]. The justification of these huge simplifications is provided at the end of this section in the context of the systemic design process of the whole microgrid (see Fig. 4). This simplified procedure uses MILP techniques on a coarse linear model of the microgrid. In this model, converter efficiencies as well as the nonlinear losses in the flywheel storage are neglected. This leads to the following simplifications:

$$\begin{cases} p_2(t) = p_3(t) \\ p_4(t) = p_5(t) \\ p_7(t) = p_8(t) \\ p_{10}(t) = p_{11}(t) \end{cases} \quad (4)$$

$$SOC(t + \Delta t) = SOC(t) - \frac{P_{st}(t) \times \Delta t}{E_{FW}} \times 100 \quad (5)$$

Taking the exceeding of subscribed power into account is strongly nonlinear. An additional integer variable δ is included in the decision variable vector [17]. The values of δ is 0 or 1 depending on either the grid power exceeds the subscribed power or not (3). It becomes possible to solve the optimal problem expressed according to (6) using Mixed Integer Linear Programming (MILP).

$$\mathbf{P^*_{ref}} = \begin{bmatrix} \mathbf{P^*_{st}} & \mathbf{P^*_{prod-c}} & \mathbf{\Delta P^*_{PV}} & \delta^* \end{bmatrix}$$
$$\mathbf{P^*_{ref}} = \arg\min(\mathbf{C_L}.\mathbf{P_{ref}}) \text{ with } \mathbf{A}.\mathbf{P^*_{ref}} \leq \mathbf{B} \quad (6)$$

The previous cost function $C(\mathbf{P_{ref}})$ is developed for the coarse model in (7) according to the decision variables P_p and P_s are linearly dependent with the degrees of freedom. The constant terms with P_{prod} and P_{load} are removed to obtain the vector $\mathbf{C_L}$ used in the MILP optimization (8) with $\mathbf{J}$ the line vector with 24 coefficient equal to 1.

$$C(\mathbf{P_{ref}}) = \sum_{t=0}^{24\text{h}} \begin{pmatrix} -P_{st}(t) \times C_c(t) + P_{prod-c}\ (\text{t}) \\ \quad \times \left(C_p(t) - C_c(t)\right) + \Delta P_{PV}(t). \times C_p(t) \\ \quad + \delta(t) \times C_{ex} + P_{load}(t) \times C_c(t) \\ \quad - P_{prod}(t).C_p(t) \end{pmatrix} \quad (7)$$

$$\mathbf{C_L}.\mathbf{P_{ref}} = C(\mathbf{P_{ref}}) - \mathbf{P_{load}} \times \mathbf{C_p^T} + \mathbf{P_{prod}} \times \mathbf{C_s^T}$$
$$\text{with } \mathbf{C}_L = \begin{bmatrix} -\mathbf{C_c^T} & (\mathbf{C_p^T} - \mathbf{C_c^T}) & \mathbf{C_c^T} & C_{ex} \times \mathbf{J} \end{bmatrix} \quad (8)$$

The constraint matrix $\mathbf{A}$ and vector $\mathbf{B}$ are built by concatenating matrices used to express each grid requirement or storage specified limits (see [16], [17] for more details). Such problem can easily be solved using a standard MILP algorithm with the GLPK solver [18]. However, one drawback of this approach resides in the fact that the optimal solution found with the MILP does not obviously comply with the requirements of the fine microgrid model. A theoric discharge down to -15 % has been observed for a tested day [17]. In the same way, the cost function returned by the coarse model is not correct. Therefore, the control references ($\mathbf{P_{ref\_LP}}$) relative to the degrees of freedom obtained with the MILP in association with the coarse model should be adapted in order to comply with the fine microgrid model. This can be performed using a step by step correction which aims at minimizing the cost while aligning the *SOC* computed from the fine model with the one resulting from the MILP optimization (denoted as SOC_{LP}). At each time step *t*, the correction procedure is formulated as in (9) to find the instantaneous optimal references $\mathbf{P^*_{ref}}(t)$ and where the $\mathbf{c^t_{nl}}$ constraint vector includes all the constraints mentioned in Section 2.1. in addition to *SOC* and power limits.

$$\mathbf{P^*_{ref}} = \begin{bmatrix} \mathbf{P^*_{st}}(t) & \mathbf{P^*_{prod-c}}(t) & \mathbf{\Delta P^*_{PV}}(t) \end{bmatrix}$$
$$\mathbf{P^*_{ref}} = \arg\min(C(\mathbf{P_{ref}}(t)))$$
$$\mathbf{c^t_{nl}}\left(\mathbf{P^*_{ref}}(t)\right) \leq 0 \text{ and } SOC(t + \Delta t) = SOC_{LP}(t + \Delta t) \quad (9)$$

This local minimization problem variables is solved using the TR method with a starting point equal to $\mathbf{P_{ref\_LP}}(t)$. The convergence is ensured in all cases in a very short CPU

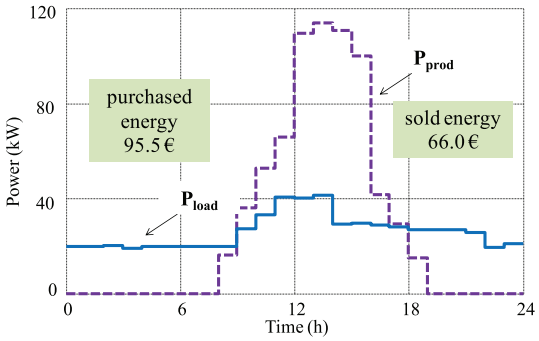

Fig. 3. Typical test day with forecasted consumption and production.

time due to its small dimensionality (only three decision variables have to be determined, the $P_{st}(t)$ decision variable being directly coupled with the *SOC* trajectory).

C. Results on a Single Test Day

These methods have been evaluated on a particular day whose characteristics are given in Fig. 3. The consumption profile $\mathbf{P_{loads}}$ extracted from data provided by the microgrid owner while the production $\mathbf{P_{prod}}$ estimation is based on solar radiation forecasts computed with a model of PV arrays [19]. Energy prices result from one of the fares proposed by the French main power supplier [20] increased by 30%. Thus, the purchase cost C_c has night and daily values with 10 c€/kWh from 10 p.m. to 6 a.m. and 17 c€/kWh otherwise. C_p is set to 10 c€/kWh which corresponds to the sale price for such PV plants. In a situation with no storage device, all the production is sold while all loads are supplied through the consumption meter. In that case, this leads to an overall cost equal to 28.5 € (Fig. 3) for the considered day. Grid constraints are established to limit the consumption during the peak hours (P_{grid_max}= 0 kW from 7 p.m. to 9 p.m.). The initial configuration of the microgrid with 156 kW subscribed power is composed of a PV generator with a peak power of 175 kW and a 100 kW/100 kWh flywheel storage.

Table II displays the energy cost obtained with all dispatching methods on the initial microgrid configuration and on the particular test day. Results show that the solution with minimum daily cost is obtained from the standard DP with an accurate discretization of the SOC level ($\Delta SOC = 1\%$). However, the corresponding CPU time of 2 h is quite expensive. The self-adaptive DP developed in [11] leads to a better compromise in terms of accuracy/computational cost by converging close to the optimal solution while significantly reducing the CPU time. In spite of this reduction, the computational cost of this method remains relatively important if we need to assess the energy cost over a complete year in order to take seasonal features into account. In that case, the CPU time related to the 365 successive dispatching steps will reach 10 min $\times$ 365 $\approx$ 3 days. In the context of the microgrid design where a second optimization loop is added for sizing the microgrid components, the CPU time will become prohibitive. Indeed, if 1000 microgrid simulations over one year are required for obtaining the optimal microgrid sizing,

TABLE II
COMPARISON OF POWER FLOW DISPATCHING STRATEGIES

Power dispatching strategy	Optimal daily cost	CPU time
TR - with 100 random initial points	0.4 €	1 h
CL - 100 individuals, 50 000 generations	0.7 €	5 h
PSO - 100 particles, 50 000 iterations	17.8 €	2 h 30 min
Standard DP - ΔSOC = 10 %	1.5 €	1 min 30 s
Standard DP - ΔSOC = 1 %	– 0.6 €	2 h
Self-adaptive DP	– 0.2 €	10 min
MILP and correction of the references	0.9 €	2 s

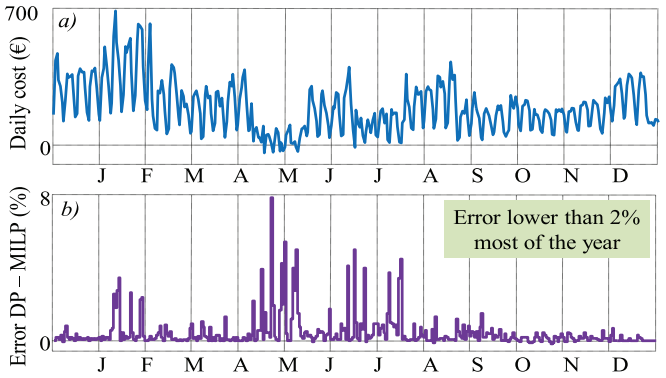

Fig. 4. Simulation over a year – *a)* Optimal daily cost – *b)* Error between MILP and self-adaptive DP results.

the CPU time will increase to 1000 $\times$3 days $\approx$ 8 years!!!. Consequently, the use of nonlinear optimization methods with the "fine" microgrid model is not suitable in the context of a design approach integrating the microgrid sizing over long periods of time. The developed approach based on the MILP and the references correction allows us to reduce the CPU over a single day to only two seconds. All the methods have been used in [17] to assess the annual cost of the components.

D. Simulation Over a Year

The previous analysis has been carried out for a single day. The reliability of the MILP approach compared to the self-adaptive DP is now controlled over a whole year. The management loop is simulated with 365 successive optimizations performed with the two methods. The input data take account of the solar radiation cycles with a geophysical model and consider the consumption variations that are computed using measurements on site. Fig. 4*a* shows the optimal daily costs returned by the self-adaptive DP algorithm. Greater electrical bills (up to 700 €) are observed during the winter months when the consumption is higher while the production remains low. Strong variations are also noticeable between the business hours and the week-end (industrial building considered). Some days correspond to negative optimal costs meaning that the sold production is favored in the energy balance with a great solar radiation. The error between the costs returned by the two optimization procedures is very low (Fig. 4*b*) and some negative values shows that in some cases the MILP algorithm

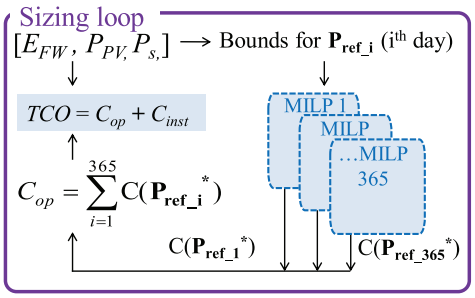

Fig. 5. Design approach of the microgrid with a bi-level optimization.

is better than the adaptive DP. The final electrical bill (without considering the investment costs) for such a representative year shows an error of 5 % depending on the used algorithm. But the management loop is simulating in only 12 min using the linear approach compared to more than 3 days with the adaptive DP.

IV. Optimal Design of the Microgrid Components

A. Bi Level Optimization

The reduced CPU time allows studying a global design approach integrating two optimization levels: energy management and sizing with regard to the microgrid environment (yearly load profiles, solar irradiation cycles) [21]. This approach is illustrated in Fig. 5 with the Total Cost of Ownership *TCO* as the sum of the operating cost C_{op} (returned by the management loop) and cost of the installation C_{inst}. In particular, we investigate the analysis and the optimization of the microgrid with regard to three design variables: the rated power P_{PV} of the PV generator, the maximum stored energy E_{FW} in the flywheels and also the subscribed power P_s to the main supplier. As in the previous section the management is daily based and the storage and the storage returns to its initial SOC level at the end of each day with an arbitrary value of 50 %. Note that a sensitivity analysis performed in [17] showed that changing that *SOC* value as well as the scheduling period (daily-based, weekly-based and monthly-based) does not have a significant effect on the final optimal yearly electrical bill.

B. Optimal Design Algorithm

The CPU time devoted to the power flow dispatching has been strongly reduced with the MILP strategy but it approximately requires 2 s × 365 ≈12 min for simulating a microgrid configuration on a complete year (with the references correction). This computational cost can be still viewed as expensive in the context of the second optimization level devoted to the microgrid sizing. In such case, the use of optimization methods based on the cost function interpolation is recommended in order to reduce the number of cost function calls. In addition, the interpolation of the objective function also returns a response surface that can be used to identify the interesting areas (i.e., with the lower annual cost here).

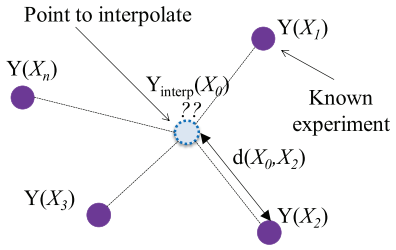

Fig. 6. Kriging interpolation.

1) Kriging Interpolation: The cost function interpolation is performed using the Kriging method [22] mainly used in geophysical applications such as the analysis of precipitation or the space localization of an ore. The Kriging is a method of interpolation for which the interpolated values are modeled by a Gaussian process. The values at the unknown points of the space are determined with the values of the known "experiments" (Fig. 6). The unknown values are expressed as a linear combination of the evaluated points (experiments):

$$Y_{interp}(X_0) = \sum_{i=1}^{n} \lambda_i \times Y(X_i) \tag{10}$$

The Kriging equations [23] aim at finding the appropriate values of the coefficients λ_i. The procedure needs a "variogram" model to compute the variance of the function depending on the distance d between the points $\gamma(d(X_0, X_i))$:

$$\mathbf{V}^{+} \cdot \boldsymbol{\lambda} = \mathbf{B}$$

$$\text{with } \mathbf{V}^{+} = \begin{bmatrix} \gamma(d(X_1,X_1)) & . & . & \gamma(d(X_1,X_n)) & 1 \\ . & & & . & . \\ . & & & . & . \\ \gamma(d(X_n,X_1)) & & & \gamma(d(X_n,X_n)) & 1 \\ 1 & . & . & 1 & 0 \end{bmatrix} \tag{11}$$

$$\boldsymbol{\lambda} = \begin{bmatrix} \lambda_1 \\ . \\ . \\ \lambda_n \\ \mu \end{bmatrix} \text{ and } \mathbf{B} = \begin{bmatrix} \gamma(d(X_0,X_1)) \\ . \\ . \\ \gamma(d(X_0,X_1)) \\ 1 \end{bmatrix}$$

$$\sigma^2(X_0) = \boldsymbol{\lambda}^{\mathbf{T}} \cdot \mathbf{B} \tag{12}$$

The procedure also returns an estimation of the error for the interpolated points (12) that allows defining a confidence interval around the interpolated function. The accuracy of the interpolation is also closely linked to the considered experimental points and to the computation of the variance with a predefined model (typically a Gaussian variation) but it is not discussed in this paper.

2) Efficient Global Optimization (EGO): The Efficient Global Optimization (EGO) algorithm [24] is used to optimize the size of the microgrid components. The algorithm estimates the cost function in unexplored points by interpolating it with the Kriging method. EGO investigates the search space by iteratively maximizing the Expecting Improvement (EI). This criterion expresses a compromise between the unexplored regions of the search space and the areas where the cost function appears to be the most interesting (i.e., with the

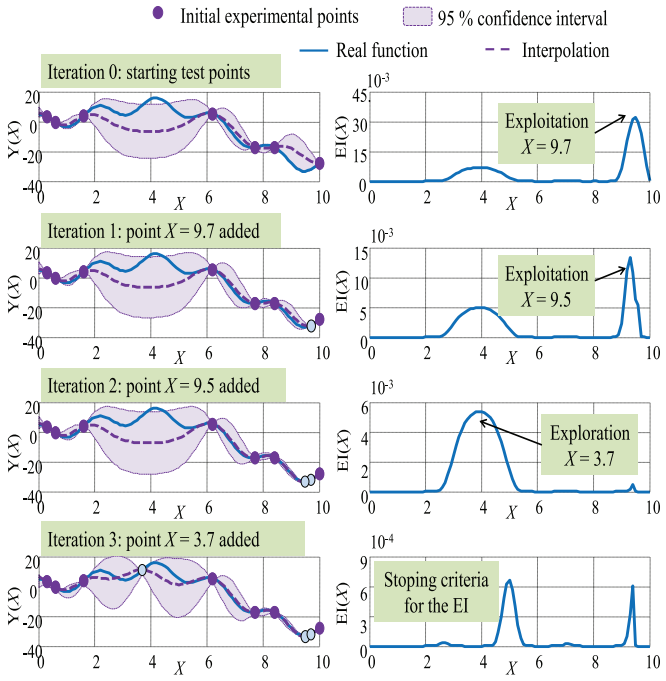

Fig. 7. Operation of the EGO on an arbitrary 1D function.

lowest values). Equation (13) shows the expression of the EI with Y_{min} the lowest known value of the function, φ the probability density function of the standard normal distribution, and Φ its cumulative probability density.

$$EI(X) = \begin{aligned} &\left(Y_{min} - Y_{interp}(X)\right) \times \Phi\left(\frac{Y_{min} - Y_{interp}(X)}{\sigma(X)}\right) \\ &+ \sigma(X) \times \varphi\left(\frac{Y_{min} - Y_{interp}(X)}{\sigma(X)}\right) \end{aligned} \quad (13)$$

Starting from randomly chosen initial test points, the method maximizes the EI at each iteration in order to find the next point that has to be evaluated. The algorithm runs until a stoping criteria is met (e.g., fixed number of iterations, no improvement on the objective function or minimum prescribed value of the EI). Fig. 7 shows the operation of the EGO for an arbitrary 1D function. The two first iterations aim at exploiting the interesting area and the optimal point X = 9.5 is found at the second step. The last iteration encourages the exploration of the search space by evaluating a point in the less known area. Finally the procedure stops beyond a minimal value of the EI (10^{-3}) meaning that no relevant improvement of the objective function should be expected.

V. Sizing Results and Return on Investment

In this section the EGO is used for the optimization of the microgrid *TCO*. The algorithm uses 10 randomly chosen starting points with a Latin Hypercube Sampling (LHS) [25]. EI is maximised using alternatively a TR method with several starting points (typically 300 points) or by regularly sampling the search space with given steps (typically 25 kWh for E_{FW}, 25 kW for P_{PV}, and 5 kVA for P_s). Those optimizations require on average 40 runs of the management loop before returning a solution. A standard genetic algorithm has been tested instead of the EGO and the returned results were not as accurate even after more than 200 evaluations of the objective function. Note that only the best point is "corrected" to comply with the requirements of the finer model. It leads to a significant reduction of the CPU time down to approximately 30 min for a single optimal sizing. In each case studies a particular attention is attached to the time of return on investment computed as follow with a lifetime of 20 years expected for the components with C_0 the cost for an initial situation with neither generation nor storage.

$$TRI = \frac{C_{inst} \times 20}{C_0 - C_{op}} \quad (14)$$

TABLE III
Optimal Points Compared to the Initial Case

	Initial case	C_p = 0 c€/kWh	C_p = 10 c€/kWh
Optimal point E_{FW}, P_{PV}, P_S	0 , 0 156	0 , 0 , 220	0, 458, 173
Storage cost (k€)	0.0	0.0	0.0
PV cost (k€)	0.0	0.0	45.8
Purchased Energy(k€)	42.7	42.6	34.3
Subscription fee (k€)	4.8	6.6	5.6
Exceed penalties (k€)	6.7	0.7	0.9
Sold energy (k€)	0.0	0.0	36.3
Taxes (k€)	24.6	24.5	20.7
TCO(k€)	**78.9**	**74.6**	**70.8**

A. Basic Price Context

The investment costs of PV generators and flywheels over the lifetime are respectively set to 2000 €/kW and 1500 €/kWh [26]. The optimal sizing is firstly performed with a basic price context corresponding to fares for industrial consumers [19]. In particular the purchase cost is very low with different values during the winter (W) from October to March and the summer (S). P_s is associated to a subscription fee of 30.7 €/kVA and taxes are equivalent to 20 % of the overall bill. With no subsidized sale for the PV production (i.e., C_p = 0 c€/kWh) the optimal sizing of the microgrid with three variables corresponds to E_{FW} and P_{PV} both equal to zero (Table III). Comparing to the initial case, the benefit are provided by the adaptation of the subscribed power. P_s is significantly increases (from 156 kVA to 220 kVA) in order to find the best compromise between the subscription fees and the penalties paid for the excess during the year. With a sale cost equal to 10 c€/kWh the optimal size for the storage remains zero while P_{PV} is close to its upper bound. The price context with a cheap purchased energy does not allow justifying the installation of a storage unit with the electrical bill not lowered enough to compensate the investment.

In a second time the optimal sizing is rerun with two variables E_{FW} and P_{PV} while P_S is set to 156 kVA. The plotted results show that the objective function (i.e., the TCO) is flat close to the optimal area with less than 1 % variation with P_{PV} values from 360 kWc to 500 kWc for the case C_s = 10 c€/kWh (Fig. 8).

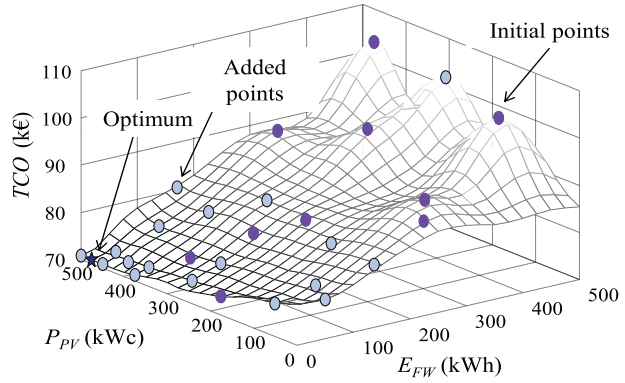

Fig. 8. Two variable optimal sizing, final interpolation for $C_s = 10$ c€/kWh.

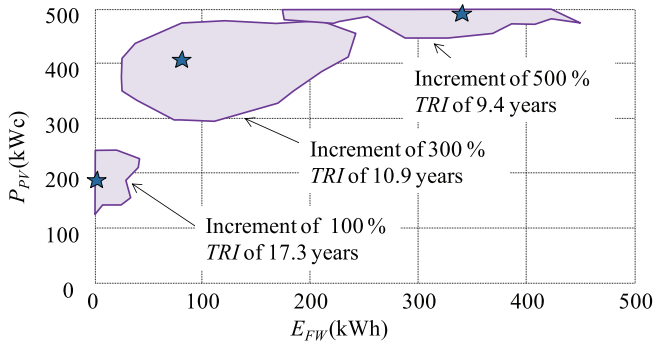

Fig. 9. Optimal results depending on the purchased prices increment.

B. Purchase Cost Increment

Purchased cost C_c and C_{ex} are now regularly increased and the two variables (E_{FW}, P_{PV}) optimization is performed to estimate when the installation of a storage device becomes interesting in a case with no sale of the production ($C_p = 0$ c€/kWh). The results of Fig. 9 show that the use of flywheel is justified with prices multiplied by three. Once again the intervals with small variations of the TCO (< 1 %) around the optimum are wide with large ranges for the values of E_{FW}. Note that the self-consumption of the PV production allows reducing the electrical bill and lowers the return on investment time. That *TRI* (for the optimal point) decreases when the purchased prices are higher with an operational cost C_0 which is more important for the initial case.

C. Derating of the Consumed Power During Peak Hours

Another service to encourage the installation of a storage unit is no considered. It consists in derating the purchased energy during the peak hour from 8 a.m. to 9 a.m. and from 7 p.m. to 9 p.m. for five months from November to March. The possibility to decrease the purchased power during peak hours is set as a constraint (for the management loop) expressed with adapted values for P_{grid_max} and a coefficient K_{der}(in %) that defines the amount of power that has to be derated. That constrained optimization is run for only one design variable E_{FW} (with P_{FW}(kW) = E_{FW}(kWh) for each flywheel sizing) while P_{PV} remains equal to zero and P_s equal to 156 kVA. Results are given in Table IV and a cost analysis is performed to estimate the total retribution with a constant

TABLE IV
COST ANALYSIS FOR THE ONE VARIABLE OPTIMIZATION

K_{der}	25 %	50 %	100 %
Optimal E_{FS}(kWh)	119.7	208.7	385.4
Storage cost (k€)	8.9	15.6	28.9
C_{der_f} retribution (k€)	6.0	10.4	19.3
C_{der_v}retribution (k€)	0.4	0.6	1.1
Overall gain (k€)	7.8	13.5	23.2

coefficient $C_{der\_f} = 50$ €/MW/year that subsidizes the rated power of the used storage and a retribution for the derated energy during the year with $C_{der\_v} = 60$ k€/kWh. The optimal size of the storage increases with the value of K_{der} with a greater amount of energy that has to be derated. For all the cases the overall gain (electrical bill reduced and retributions) compared to the initial case is computed with the reduction of the electrical bill (purchased energy and exceeding of P_s) and the retribution according C_{der_f} and C_{der_v}. In the considered price context that gain does not compensate the annual investment cost for the flywheels. Note that the constant cost of the installed power is much higher than the retribution of the derated energy.

D. Optimization of the Price Context

In that subsection the sizing approach coupled with the management strategy developed in the paper is used to optimize the price context. The goal is to obtain a given TRI denoted as TRI_{expect} for fixed values of E_{FW}, P_{PVnom} and P_s. Thus the design variables are all the costs that intervene in the price policy. To limit the number of parameters, four variables are identified with the bounds specified in (15) and with $K_{\%}$ the increment of the basic purchased cost (as in Section V.B).

$$\begin{aligned} &0\ \% \le K_{\%} \le 200\ \% \\ &0\ \text{c€/kWh} \le C_p \le 20\ \text{c€/kWh} \\ &0\ \text{k€/MW/year} \le C_{der\_f} \le 100\ \text{k€/MW/year} \\ &0\ \text{k€/kWh} \le C_{der\_v} \le 120\ \text{k€/kWh} \end{aligned} \tag{15}$$

The objective function expressed as in (16) is the error between the obtain TRI and the expected value and the optimum is obtained when f_{obj} equals zero.

$$f_{obj} = \left(TRI - TRI_{expect}\right)^2 \tag{16}$$

The solution is not unique as several fares may lead to the same *TRI*. Thus Table V shows different price context that corresponds with a TRI of ten years for an installation characterized by E_{FW}= 100 kWh (P_{FW}=100 kW) and $P_{PV} = 100$ kWc. P_s is set to 200 kVA and the management loop is run with $K_{der} = 30$ %. All the solutions correspond to an increment of the purchased prices that have to be doubled at least. Note that the actual purchase cost of electricity from grid C_c (with no taxes) remains very low with 3 or 4 c€/kWh during summer. For a moderate increment (150 %) the sale of the PV production should be highly subsidized with C_p equal to the upper bound at 20 c€/kWh. The retributions of the installed storage C_{eff_f} and C_{eff_v} must be higher than the

TABLE V
PRICE CONTEXT THAT ENSURES THE EXPECTED TRI

	$K_{\%}$ (%)	C_p (c€/kWh)	C_{eff_f} (k€/MW/year)	C_{eff_v} (k€/kWh)
Solution 1	179.9	8.3	87.0	94.0
Solution 2	198.1	2.4	77.3	67.1
Solution 3	150.0	20.0	70.0	50.0
Solution 4	200.0	1.8	60.0	80.0

values considered in Section V.C in order to compensate the investment cost of the storage device.

VI. CONCLUSION

In this paper, a global integrated design approach for the energy management and sizing of a microgrid with storage has been presented. The studied microgrid is composed of commercial buildings and factories that include PV production and flywheel storage. In a first part of the paper, several power flow dispatching strategies based on nonlinear optimization techniques have been compared in terms of efficiency and CPU time. All those methods can be used for predicting for the day ahead the optimal references of the power flows but they are too expensive in the case of the microgrid simulation over a long period of time (typically one year). Furthermore several wide horizon simulations are required in the context of a second optimization step related to the microgrid component sizing taking seasonal variations into account. To face this problem an original fast power flow dispatching approach has been presented. This approach relies on the use of MILP techniques in association with a coarse linear model of the microgrid in order to speed up the computational time. Then, a correction procedure is applied for aligning the results of the coarse model with the finer nonlinear model. This approach has shown to be highly effective leading to a significant reduction of the computational time of the power flow scheduling. In the following part of the paper, a second optimization level has been introduced aiming at finding the optimal microgrid configuration with regard to different design variables (energy management variables and sizing variables). The developed method based on Kriging interpolation has been explained with an illustration given for a 1D arbitrary function. Finally the developed approach is very fast with optimal designs performed in around 30 min if the references of the power flows are corrected only for the final solution. The fast computational time allows running many optimization problems with different formulation (constraints, optimization of the TRI) and various price contexts. The obtained results show that with the actual policy the investments for a storage unit cannot be compensated by the reduction of the electrical bill. If the TRI becomes interesting for a great increment of the purchased costs other services such as derating of the consumed power could be subsidized to favor the installation of storage devices. The implemented tool revealed itself very efficient with fast computational time and allows to consider various kind of problems such as optimal sizing or optimal price context.

REFERENCES

[1] G. Celli *et al.*, "Meshed vs. radial MV distribution network in presence of large amount of DG," in *Proc. IEEE PES Power Syst. Conf. Expo.*, New York, NY, USA, 2004, pp. 709–714.

[2] S. Yeleti and Y. Fu, "Impacts of energy storage on the future power system," in *Proc. North Amer. Power Symp. (NAPS)*, Arlington, TX, USA, 2010, pp. 1–7.

[3] C. M. Colson and M. H. Nehrir, "A review of challenges to real-time power management of microgrids," in *Proc. IEEE Power Energy Soc. Gen. Meeting*, Calgary, AB, Canada, 2009, pp. 1–8.

[4] H. K. Fathy, J. A. Reyer, P. Y. Papalambros, and A. G. Ulsoy, "On the coupling between the plant and controller optimization problems," in *Proc. Amer. Control Conf.*, Arlington, TX, USA, 2001, pp. 1864–1869.

[5] R. Rigo-Mariani *et al.*, "Off-line and on-line power dispatching strategies for a grid connected commercial building with storage unit," in *Proc. 8th IFAC Power Plant Power Syst. Control*, Toulouse, France, 2012.

[6] H. Kanchev, D. Lu, F. Colas, V. Lazarov, and B. Francois, "Energy management and operational planning of a microgrid with a PV-based active generator for smart grid applications," *IEEE Trans. Ind. Electron.*, vol. 58, no. 10, pp. 4583–4592, Oct. 2011.

[7] M. Korpaas, A. T. Holen, and R. Hildrum, "Operation and sizing of energy storage for wind power plants in a market system," *Int J. Elect. Power Energy Syst.*, vol. 25, no. 8, pp. 599–606, 2003.

[8] T. Malakar, S. K. Goswami, and A. K. Sinha, "Optimum scheduling of micro grid connected wind-pumped storage hydro plant in a frequency based pricing environment," *Int J. Elect. Power Energy Syst.*, vol. 54, pp. 341–351, Jan. 2014.

[9] P. Pankovits *et al.*, "Design and operation optimization of a hybrid railway power substation," in *Proc. 15th Eur. Conf. Power Electron. Appl. (EPE)*, Lille, France, 2013, pp. 1–8.

[10] S. Bolognani, G. Cavraro, F. Cerruti, and A. Costabeber, "A linear dynamic model for microgrid voltages in presence of distributed generation," in *Proc. IEEE 1st Int. Workshop Smart Grid Model. Simulat. (SGMS)*, Brussels, Belgium, 2011, pp. 31–36.

[11] R. Rigo-Mariani, B. Sareni, X. Roboam, and C. Turpin, "Optimal power dispatching strategies in smart-microgrids with storage," *Renew. Sustain. Energy Rev.*, vol. 40, pp. 649–658, Dec. 2014.

[12] T. F. Coleman and Y. Li, "An interior trust region approach for nonlinear minimization subject to bounds," *SIAM J. Optim.*, vol. 6, no. 2, pp. 418–445, 1996.

[13] R. C. Eberhart and J. Kennedy, "A new optimizer using particle swarm theory," in *Proc. 6th Int. Symp. Micromach. Human Sci.*, Nagoya, Japan, 1995, pp. 39–43.

[14] A. Pétrowski, "A clearing procedure as a niching method for genetic algorithms," in *Proc. IEEE Int. Conf. Evol. Comput.*, Nagoya, Japan, 1996, pp. 798–803.

[15] D. P. Bertsekas, *Dynamic Programming and Optimal Control*, 2nd ed. Belmont, MA, USA: Athena Scientific, 2000.

[16] R. Rigo-Mariani, B. Sareni, and X. Roboam, "A fast optimization strategy for power dispatching in a microgrid with storage," in *Proc. 39th Annu. Conf. IEEE Ind. Electron. Soc.*, Vienna, Austria, 2013, pp. 7902–7907.

[17] R. Rigo-Mariani, B. Sareni, and X. Roboam, "Fast power flow scheduling and sensitivity analysis for sizing a micorgrid with storage," in *Proc. 11th Int. Conf. Model. Simulat. Elect. Mach. Converters Syst. (ELECTRIMACS)*, Valencia, Spain, May 2014.

[18] B. Meindl and M. Templ, "Analysis of commercial and free and open source solvers for linear optimization problems," Dept. Inst. Statist., Vienna Univ. Technol., Vienna, Austria, Tech. Rep. CS-2012-1, 2012.

[19] C. Darras *et al.*, "Sizing of photovoltaic system coupled with hydrogen/oxygen storage based on the ORIENTE model," *Int. J. Hydrogen Energy*, vol. 35, no. 8, pp. 3322–3332, 2010.

[20] (Jan. 2015). *Electricité de France Website*. [Online]. Available: http://france.edf.com

[21] J. W. Whitefoot, A. R. Mechtenberg, D. L. Peters, and P. Y. Papalambros, "Optimal component sizing and forward-looking dispatch of an electrical microgrid for energy storage planning," in *Proc. Int. Design Eng. Tech. Conf. Comput. Inf. Eng. Conf.*, Washington, DC, USA, 2011, pp. 341–350.

[22] G. Matheron, "Principles of geostatistics," *Econ. Geol.*, vol. 58, no. 8, pp. 1246–1266, 1963.

[23] M. Borga and A. Vizzaccaro, "On the interpolation of hydrologic variables: Formal equivalence of multiquadratic surface fitting and kriging," *J. Hydrol.*, vol. 195, nos. 1–4, pp. 160–171, 1997.

[24] D. R. Jones, M. Schonlau, and W. J. Welch, "Efficient global optimization of expensive black-box functions," *J. Global Optim.*, vol. 13, no. 4, pp. 455–492, 1998.
[25] M. D. Mckay, R. J. Beckman, and W. J. Conover, "A comparison of three methods for selecting values of input variables in the analysis of output from a computer code," *Technometrics*, vol. 42, no. 1, pp. 55–61, 2000.
[26] (Jan. 15). *Beacon Power Website*. [Online]. Available: http://www.beaconpower.com

Remy Rigo-Mariani was born in Ajaccio, France. He received the M.S. degree in electrical engineering and the Ph.D. degree from the Institut National Polytechnique de Toulouse, France, in 2009 and 2014, respectively. He is currently a Postdoctoral Fellow with the Renewable Energy Analysis Laboratory, University of Washington, Seattle. His research interests refer to power systems modeling/analysis, optimal management, and design for microgrid mixing renewable energy sources and storage units.

Bruno Sareni was born in Bron, France, in 1972. He received the Ph.D. degree from École Centrale de Lyon, Écully, France, in 1999. He is currently a Professor in Electrical Engineering and Control Systems with the National Polytechnic Institute of Toulouse, Toulouse, France. He is also a Researcher with the Laboratory on Plasma and Conversion of Energy, Université de Toulouse, Toulouse. His research interests include integrated design approaches for electrical embedded systems or renewable energy systems.

Xavier Roboam received the Ph.D. degree in electrical engineering from the Institut National Polytechnique de Toulouse, Toulouse, France, in 1991. He is a Senior Scientist CNRS and Full-Time Researcher with the Laboratory on Plasma and Conversion of Energy, Université de Toulouse, Toulouse. He is engaged in developing methodologies specifically oriented toward multifields systems design for applications such as electrical embedded systems or renewable energy systems.